


Lipid transfer protein StLTPa enhances potato disease resistance against different pathogens by binding and disturbing the integrity of pathogens plasma membrane

Xiaokang Chen¹, Jiashu Feng¹, Zhenzhen Li¹, Hui Feng², Chunxu Song^{3,4}, Lin Cai², Matthieu H. A. J. Joosten⁵ and Yu Du^{1,*} 

¹State Key Laboratory for Crop Stress Resistance and High-Efficiency Production and College of Horticulture, Northwest A&F University, Yangling, China

²College of Tobacco Science of Guizhou University/Key laboratory of Plant Resource Conservation and Germplasm Innovation in Mountainous Region (Ministry of Education)/Guizhou Key Lab of Agro-Bioengineering, Guiyang, China

³State Key Laboratory of Nutrient Use and Management, College of Resources and Environmental Sciences, China Agricultural University, Beijing, China

⁴National Academy of Agriculture Green Development, China Agricultural University, Beijing, China

⁵Laboratory of Phytopathology, Wageningen University, Wageningen, The Netherlands

Received 3 July 2023;

revised 20 January 2024;

accepted 2 February 2024.

*Correspondence (Tel (0086)029-87082613; fax (0086)029-87082613; email yu.du@nwfau.edu.cn)

Summary

Potato is the third most important food crop worldwide. Potato production suffers from severe diseases caused by multiple detrimental plant pathogens, and broad-spectrum disease resistance genes are rarely identified in potato. Here we identified the potato non-specific lipid transfer protein StLTPa, which enhances species non-specific disease resistance against various pathogens, such as the oomycete pathogen *Phytophthora infestans*, the fungal pathogens *Botrytis cinerea* and *Verticillium dahliae*, and the bacterial pathogens *Pectobacterium carotovorum* and *Ralstonia solanacearum*. The StLTPa overexpression potato lines do not show growth penalty. Furthermore, we provide evidence that StLTPa binds to lipids present in the plasma membrane (PM) of the hyphal cells of *P. infestans*, leading to an increased permeability of the PM. Adding of PI(3,5)P₂ and PI(3)P could compete the binding of StLTPa to pathogen PM and reduce the inhibition effect of StLTPa. The lipid-binding activity of StLTPa is essential for its role in pathogen inhibition and promotion of potato disease resistance. We propose that StLTPa enhances potato broad-spectrum disease resistance by binding to, and thereby promoting the permeability of the PM of the cells of various pathogens. Overall, our discovery illustrates that increasing the expression of a single gene in potato enhances potato disease resistance against different pathogens without growth penalty.

Keywords: *Phytophthora infestans*, broad-spectrum disease resistance, plant immunity.

Introduction

Potato is one of the most essential food crops worldwide (Zhang *et al.*, 2017). However, its production suffers from severe diseases caused by multiple detrimental plant pathogens. For example, the oomycete pathogen *Phytophthora infestans* is responsible for the widespread and economically detrimental late blight disease, resulting in substantial annual losses in potato production worldwide. So far, breeding strategies for potato disease resistance heavily rely on race-specific disease resistance genes, which are easily overcome by the appearance of new strains of the pathogen. Consequently, the development of potato cultivars with durable and broad-spectrum resistance (BSR; Hao *et al.*, 2022) is recognized as the most sustainable way to secure potato production. BSR encompasses two types of resistance: species-specific (SS) and species-non-specific (SNS) resistance, with SS BSR conferring resistance against a specific pathogen, while SNS BSR confers resistance against more than two different pathogens (Ke *et al.*, 2017). Currently, there are two common ways to improve crop BSR, which is by stacking multiple disease

resistance genes (Ghislain *et al.*, 2019) and by knocking out of susceptibility genes (Sha *et al.*, 2023; Wang *et al.*, 2022). However, these two ways are either technically difficult to perform or it results in resistant crops showing growth and yield penalties, which hampers their utilization in food production.

The extracellular space of plants, also known as the apoplast, acts as the front line in plant-pathogen interactions (Du *et al.*, 2016). After pathogen ingress into the apoplast, plants have been shown to secrete a plethora of defence-related proteins to fend off the invading pathogen, including, amongst others, immune-related proteases, glucanases, chitinases and additional pathogenesis-related (PR) proteins (Joosten and De Wit, 1989). Some of these defence-related apoplastic proteins have reported to have antimicrobial activities.

nsLTPs are encoded by a large gene family, and are cysteine-rich proteins with molecular weights ranging from 6.5 to 10 kDa and their presence is widely distributed over all higher plants. nsLTPs bind to, and transport, various lipids, and have reported to participate in plant growth and development, seed development and germination and plant resistance to biotic and abiotic stresses

Please cite this article as: Chen, X., Feng, J., Li, Z., Feng, H., Song, C., Cai, L., Joosten, M H A J. and Du, Y. (2024) Lipid transfer protein StLTPa enhances potato disease resistance against different pathogens by binding and disturbing the integrity of pathogens plasma membrane. *Plant Biotechnol. J.*, <https://doi.org/10.1111/pbi.14310>.

(Gao et al., 2022). For example, wheat (*Triticum aestivum*) TaLTP4 is produced in response to both biotic and abiotic stresses (Safi et al., 2015), and potato StLTP1 and StLTP7 were reported to enhance potato drought stress tolerance (Wang et al., 2023). *Brassica rapa* BrLTP2.1 shows antifungal activities (Schmitt et al., 2018), whereas *Arabidopsis thaliana* AtLTP4.4 shows antifungal activity, and overexpression of AtLTP4.4 or its wheat homologue TaLTP3, increases wheat resistance to the pathogenic fungus *Fusarium graminearum* (McLaughlin et al., 2021). However, *Arabidopsis* AtLTP3 was found to negatively regulate plant resistance to *Pseudomonas syringae* pv. *tomato* (*Pst*) DC3000 (Gao et al., 2016), which indicates that plant nsLTPs may play diverse roles in the response of plants to pathogens. Whether StLTPs in potato have anti-oomycete activity and whether StLTPs enhance potato immunity to multiple detrimental plant pathogens, especially the notorious late blight disease, remains to be shown.

Here we identified a potato StLTPa protein that enhances potato species none-specific broad-spectrum disease resistance against oomycete, fungal and bacterial pathogens. *In vitro* assays show that StLTPa inhibits the proliferation of oomycetes, fungi and bacteria, and the protein binds to lipids that are present on the plasma membrane (PM) of the cells of pathogens. Lipid-binding activity of StLTPa is required for promoting the permeability of the PM and enhancing potato SNS BSR. Our research provides evidence that increasing the expression level of a single gene enhances crop broad spectrum disease resistance.

Results

Identification of secreted defence-related StLTPs proteins from *Nicotiana benthamiana* and potato

To identify defence-related apoplastic proteins, *Nicotiana benthamiana* leaves were inoculated with *P. infestans* zoospores. Apoplastic fluid was subsequently extracted at 0 and 24 h post-inoculation for analysis by mass spectrometry. Six NbLTP proteins were identified in the apoplast of *N. benthamiana* leaves at 24 h after *P. infestans* inoculation (Figure S1; Table S1). To determine whether these LTPs play a role in plant immunity, we transiently expressed the six NbLTPs, and the control SP-GFP consisting of GFP fused to the signal peptide for extracellular targeting of NbLTPa, in leaves of *N. benthamiana*, and performed detached leaf inoculation assays. We observed that all NbLTPs-expressing leaves developed significantly smaller lesions than the SP-GFP-expressing leaves. In particular, the expression of NbLTPa (*Niben101Scf12307g01004*) and NbLTPb (*Niben101Scf07809g00010*) inhibited lesion expansion to a greater extent than the other four NbLTPs. (Figure S2). We selected NbLTPa and NbLTPb, providing a stronger resistance to potato late blight, for further studies. To further confirm the function of these NbLTPs in disease resistance, we silenced *NbLTPa* & *-b* by virus-induced gene silencing (VIGS), using recombinant tobacco rattle virus (TRV), and again performed *P. infestans* inoculation assays. The TRV-*NbLTP*-inoculated plants developed significantly larger lesions when compared to the control, TRV-*GUS*-inoculated, plants, indicating that these two NbLTPs do play a positive regulatory role in plant immunity (Figure S3).

To investigate the role of LTPs in potato immunity to *P. infestans*, we cloned the homologous genes of *NbLTPa* and *NbLTPb* of potato, referred to as *StLTPa* (PGSC0003DMC400054441), *StLTPb* (PGSC0003DMC400003396), and *StLTPc* (PGSC0003DMC400021169), from the potato cultivar 'Desiree' according to the phylogenetic tree analysis of LTP proteins from potato, tomato,

N. benthamiana, pepper, *A. thaliana* and *Oryza sativa* (Figure S4). Multiple sequence alignments show that the key motifs of the various LTPs in potato, tomato, *N. benthamiana* and *A. thaliana* are conserved (Figure S5). *StLTPa/b/c* were transiently expressed in leaves of *N. benthamiana* and at 1 day post infiltration, zoospores of *P. infestans* were inoculated onto the infiltrated leaves. We again observed that transient expression of *StLTPa*, *StLTPb*, and *StLTPc* enhances *N. benthamiana* immunity to *P. infestans* and now the *StLTPa*-expressing plants show the strongest increase in resistance to *P. infestans* (Figure S6). Thus, we chose *StLTPa* for further study.

StLTPa promotes potato resistance to *P. infestans*

To analyse the role of *StLTPa* in resistance of potato, we generated five independent transgenic lines (referred to as *StLTPa*-1, -2, -3, -4, -5) with increased *StLTPa* expression, and two independent *StLTPa*-RNAi lines (referred to as RNAi-8, RNAi-11) with decreased expression of *StLTPa*, in potato cultivar Desiree (Figure S7a–g). We observed a faster development of the plants expressing *StLTPa*, at 2 weeks after planting when compared to the wild-type Desiree control, while the *StLTPa*-silenced potato transgenic lines showed slight developmental defects (Figure S7a,d,f).

To further analyse the role of *StLTPa* in potato immunity to *P. infestans*, we inoculated the *StLTPa*-overexpressing (OE) lines and *StLTPa*-RNAi lines with *P. infestans*. We observed that all five *StLTPa*-OE lines show enhanced immunity to different isolates (14-3-GFP and 88069) of *P. infestans* (Figure 1a–d; Figure S7h,i). Whole plant spray inoculations also showed that the *StLTPa*-OE lines are more resistant to *P. infestans* than the Desiree control (Figure 1e,f). In contrast, the *StLTPa*-RNAi lines showed compromised resistance to *P. infestans* when compared with the wild-type Desiree control (Figure 1g,h). To investigate whether the *StLTPa* gene is transcriptionally regulated during the response of potato to inoculation with *P. infestans*, we determined the expression pattern of *StLTPa* in the *P. infestans*-susceptible and -resistant cultivars Desiree and Qingshu 9, respectively, during the early stages after pathogen inoculation. The qRT-PCR results show that the expression of *StLTPa* is significantly induced upon *P. infestans* inoculation in both potato cultivars, and that *StLTPa* expression reached its peak at 3 h after inoculation. In addition, we observed that the expression of *StLTPa* is more strongly induced in the resistant potato cultivar Qingshu 9 than in susceptible Desiree plants at 3 hpi (Figure S8).

StLTPa overexpressing potato plants show broad-spectrum disease resistance to multiple pathogens

To verify whether the *StLTPa*-OE lines also have an enhanced SNS BSR, the fungal pathogens *Botrytis cinerea*, which is a necrotrophic pathogen that causes grey mould, and *Verticillium dahliae* that causes vascular wilt of potato, were inoculated on either the leaves or the roots, respectively, of the different potato lines. The results show that the various *StLTPa*-OE lines display significantly smaller lesions on their leaves when inoculated with *B. cinerea* and less wilt upon *V. dahliae* inoculation, when compared to the wild-type Desiree plants, while the *StLTPa*-RNAi lines display significantly larger lesions on their leaves when inoculated with *B. cinerea* (Figure 2a–d; Figure S9a,b). To further confirm the role of *StLTPa* in SNS BSR, we inoculated the different *StLTPa*-OE lines with the bacterial pathogens *Pectobacterium carotovorum* and *Ralstonia solanacearum*, which cause blackleg and bacterial wilt on potato, respectively. Our results show that the overexpression of *StLTPa* also enhances potato immunity to

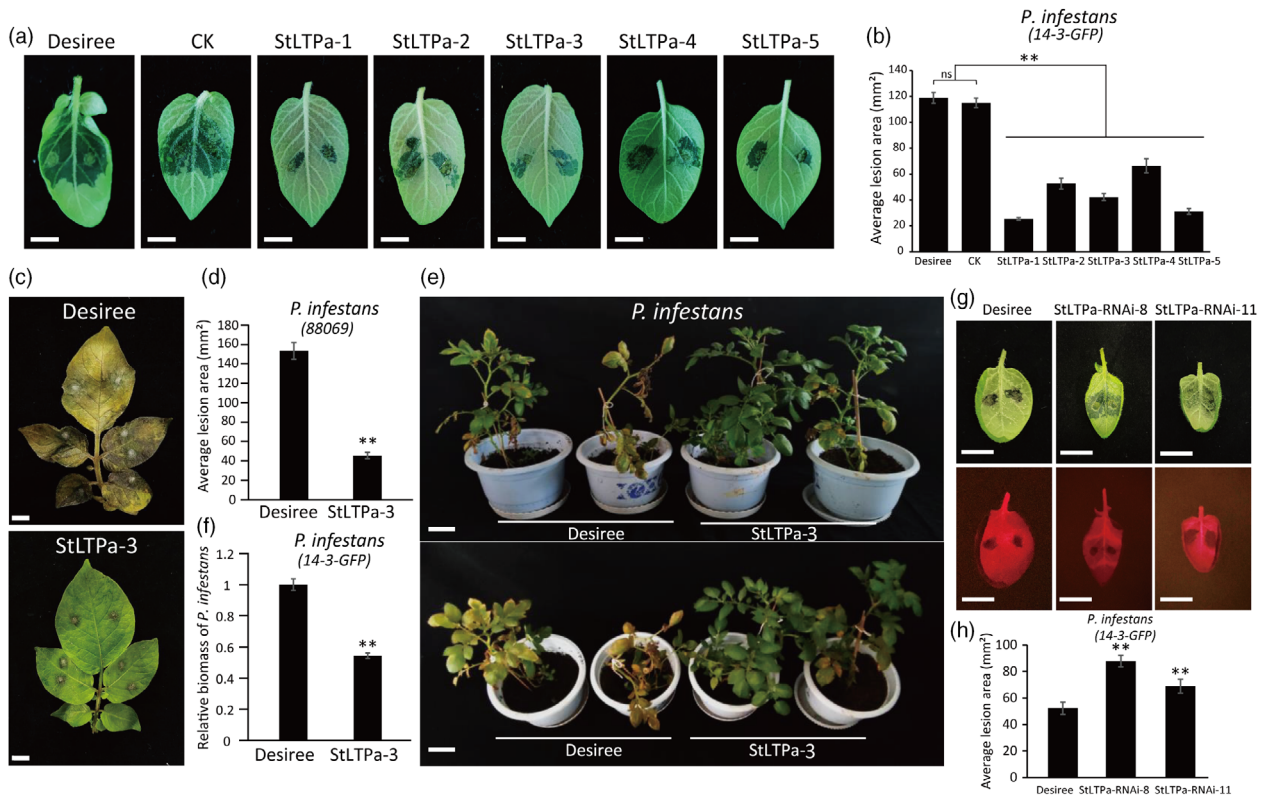


Figure 1 StLTPa over expression (OE) enhances plant immunity to *P. infestans*. (a) Representative images showing *P. infestans* strain 14-3-GFP lesion development on leaves of wild-type (WT) Desiree and StLTPa-OE-transgenic lines at 4 days after inoculation (dai), CK, transformant with no DNA inserts. (b) Bar graph showing the average lesion areas on all inoculated leaves from the lines shown in (a). Error bars show the standard errors (one-sided Student's *t*-test, $**P < 0.01$; $n = 10$). (c) Representative images showing symptoms of a compound leaf inoculated with zoospores of *P. infestans* strain 88069 from Desiree and a StLTPa-3 OE line. The pictures were taken at 5 dai. (d) Bar graph showing the average lesion areas on all inoculated leaves from the lines shown in (c). Error bars indicate the standard errors (one-sided Student's *t*-test, $**P < 0.01$; $n = 28$). Scale bars for (a) and (c), 1 cm. (e) Phenotypes of Desiree and the StLTPa-3 line that were spray-inoculated with zoospores of *P. infestans* strain 14-3-GFP. Pictures were taken at 10 dai. Scale bars, 5 cm. (f) Bar graph showing the relative biomass of *P. infestans* in the lines shown in (e), as determined with quantitative reverse transcription qRT-PCR, at 10 dai. Bars represent *P. infestans* strain 14-3-GFP ITS levels, relative to potato *Stactin* gene expression levels, with standard deviation, in a sample of three pooled plants. Above experiments were repeated three times, with similar results. (g) Representative images showing *P. infestans* strain 14-3-GFP lesion development on leaves of WT Desiree and StLTPa-RNAi-transgenic lines at 4 days after inoculation (dai). Scale bars, 1 cm. (h) Bar graph showing the average lesion areas on all inoculated leaves from the lines shown in (g). Error bars show the standard errors (one-sided Student's *t*-test, $**P < 0.01$; $n = 10$). The experiments were repeated at least two times, with similar results.

both bacterial pathogens, whereas the StLTPa-RNAi plants showed compromised resistance to *Ralstonia solanacearum* (Figure 2e–h; Figure S9c,d).

Recombinant StLTPa protein exhibits broad-spectrum antimicrobial activity

Since StLTPa contains a signal peptide for extracellular targeting, we speculated that it may be secreted into the apoplast of the plant. We isolated apoplastic fluids from *N. benthamiana* leaves transiently expressing StLTPa-GFP and were able to detect the protein in an apoplastic extract (Figure S10), indicating that it is indeed secreted protein. Since it has been reported previously that AtLTP4.4 shows antifungal activity, we decided to investigate whether potato StLTPa also has antimicrobial activity. We purified the GST-GFP control, GST-StLTPa (StLTPa without signal peptide) and GST-StLTPa^{3A} (GST-StLTPa^{R67A,Y102A,I104A}), StLTPa without signal peptide and with a mutation of three essential amino acids in its lipid-binding domain (Cheng *et al.*, 2004; Lee *et al.*, 1998) from *Escherichia coli* cell, heterologously producing the protein *in vitro*, and incubated the proteins with zoospores from *P. infestans*

and *P. capsici*, and with spores from *B. cinerea*, at a concentration of 5 μM . Five hours after incubation, we observed that in the GST-GFP- and GST-StLTPa^{3A}-treated samples, the zoospores and spores from either the *Phytophthora* pathogens or *Botrytis* started to germinate, whereas in the GST-StLTPa-treated samples there was no germination observed (Figure 3a–d). In addition, the GST-StLTPa treated *P. infestans* zoospores fail to form lesions on leaves of *N. benthamiana*, while GST-StLTPa^{3A} and GST-GFP treated zoospores formed lesions (Figure 3e,f). This inhibition of germination indicates that StLTPa indeed has antimicrobial activity. To further confirm this, we determined mycelial growth of *P. infestans*, *P. capsici* and *B. cinerea* on rye and sucrose agar (RSA), CA and PDA solid medium, respectively, in the presence of 5 μM GST-StLTPa protein. Our results show that GST-StLTPa, but not the GST-StLTPa^{3A} mutant, significantly inhibits hyphal growth of *P. infestans* and *P. capsici* and weakly inhibits hyphal growth of *B. cinerea* (Figure 3g–j). Proliferation of the bacterial pathogens *P. carotovorum* and *R. solanacearum* were also inhibited by a 5 μM concentration of the GST-StLTPa protein (Figure 3k,l). To further confirm the broad antimicrobial activity of StLTPa, we

4 Xiaokang Chen et al.

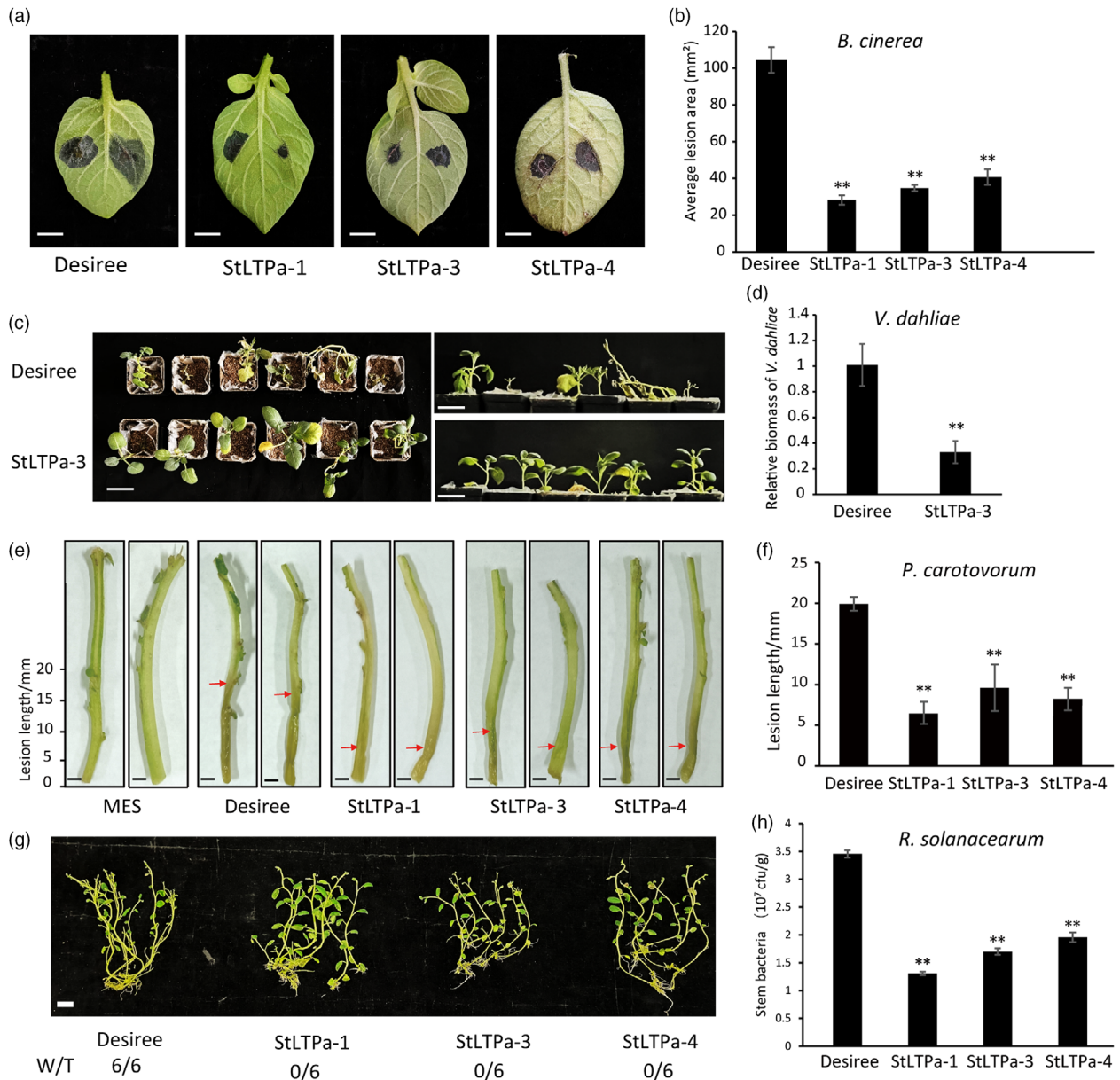


Figure 2 StLTPa confers broad spectrum disease resistance in potato. (a) Representative images showing lesion development on leaves of Desiree and StLTPa-OE lines that were inoculated with *Botrytis cinerea*, at 2 dpi. Scale bar, 1 cm. (b) Bar graph showing the average lesion areas on all inoculated leaves from the lines shown in (a). Error bars show the standard errors, asterisks indicate significant differences (one-sided Student's *t*-test, $**P < 0.01$; $n \geq 20$). (c) Typical disease symptoms of Desiree and StLTPa-OE-transgenic lines upon inoculation with *V. dahliae*, at 21 dai. Scale bars, 5 cm. (d) Bar graph showing the relative biomass of *V. dahliae* in the lines shown in (c), as determined with real-time PCR at 21 dai. Bars represent *V. dahliae* ITS levels relative to potato *Stactin* gene expression levels, with standard deviation, in a sample of six pooled plants. One-sided Student's *t*-tests were used to assess significance, $**P < 0.01$. (e) Representative images showing *P. carotovorum* lesion development on detached petioles of StLTPa-OE potato lines and the control Desiree at 2 dpi. Scale bar, 200 mm. (f) Bar graph showing the average lesion length caused upon inoculation with *P. carotovorum* of the lines shown in (e). Statistical analysis was performed using one-sided Student's *t*-test ($**P < 0.01$, $n = 7$). Error bars represent the standard errors. (g) Representative images showing wilt symptoms in wild-type Desiree and StLTPa-OE lines upon inoculation with *R. solanaceum*. W/T indicates the number of wilted plants with respect to the total number of inoculated plants. Scale bar, 1 cm. (h) Statistical analysis of the colonization levels by *R. solanaceum* of the stems of the lines shown in (g). Two-week-old potato plants were inoculated with *R. solanaceum* by the hydroponic inoculation method and photographed at 5 dai. Error bars show the standard deviations from six replicates. Two-sided Student's *t*-tests were used to assess significance: $**P < 0.01$. The experiments were repeated three times with similar results.

inoculated GST-StLTPa- or GST-GFP-treated *P. capsici* and *B. cinerea* zoospores onto leaves of *N. benthamiana* and observed that the GST-StLTPa-treated zoospores cause smaller lesions than the GST-GFP control (Figure S11). Taken together, these results

indicate that StLTPa exerts antimicrobial activity towards oomycete, fungal and bacterial pathogens, which explains why its overexpression causes resistance to infection by different types of pathogens.

StLTPa binds to various lipids and is able to enhance the permeability of the PM of the cells of pathogens

To further investigate the mechanism behind the antimicrobial activity of StLTPa, we first determined whether StLTPa directly binds to the oomycete PM. For this, protoplasts of *P. infestans* and potato, as a control, were incubated with GST-StLTPa and GST-StLTPa^{3A} and the PM fraction was subsequently obtained. GST-StLTPa, but not GST-StLTPa^{3A}, was more abundant in the PM fraction than in the cytosolic fraction of the *P. infestans* protoplasts and in the supernatant collected through centrifugation after the incubation, indicating binding of StLTPa to the PM of *P. infestans*. However, both GST-StLTPa and GST-StLTPa^{3A} were more abundant in the supernatant of the potato protoplasts, indicating that both GST-StLTPa and GST-StLTPa^{3A} do not bind to the PM of potato cells (Figure 4a–d). Furthermore, we checked whether StLTPa binds to various lipids and if so, to which types of lipids it does bind to. The results of lipid blot assays revealed that StLTPa strongly binds to phosphatidylinositol (3,5)-bisphosphate (PtdIns(3,5)P₂ or PI(3,5)P₂), phosphatidylinositol (3)-phosphate (PtdIns(3)P or PI(3)P). Furthermore, it binds weakly to phosphatidylinositol (4)-phosphate (PtdIns(4)P, or PI(4)P), phosphatidylinositol (5)-phosphate (PtdIns(5)P, or PI(5)P), phosphatidylinositol (4,5)-bisphosphate (PtdIns(4,5)P₂ or PI(4,5)P₂), phosphatidylinositol (3,4,5)-triphosphate (PtdIns(3,4,5)P₃ or PI(3,4,5)P₃) and phosphatidic acid (PA). Interestingly, we observed that the GST-StLTPa^{3A} mutant has completely lost its lipid-binding activity (Figure 4e). To investigate whether the lipid-binding activity is related to mediating disease resistance and StLTPa antimicrobial activity, we again performed pathogen inoculations and mycelium growth inhibition assays and observed that StLTPa^{3A} has not only lost the ability to enhance resistance to *P. infestans*, but also has lost the ability to inhibit mycelial growth of *P. infestans* (Figure S12; Figure 3g,h). Since the lipid binding activity of StLTPa appears to play an essential role in pathogen inhibition, we hypothesized that StLTPa might inhibit pathogen proliferation by binding to, and thereby disrupting, the PM of the cells of the invading pathogen. To proof this, we verified whether retention of the StLTPa protein takes place by the major components of the oomycete PM, which are phosphatidylethanolamine (PE), 1,2-dipalmitoyl-sn-glycero-3-phosphocholine (DPPC), 1,2-dioleoyl-sn-glycero-3-phosphocholine (DOPC), and sphingomyelin (SM). Concerning the fungal PM, the main component ergosterol was taken along, and cell walls of *P. infestans* were used as a control. The above-mentioned components were individually coated onto glass discs and then air-dried. Subsequently, they were covered with GST-StLTPa and the negative control GST-StLTPa^{3A}. Interestingly, the StLTPa protein is retained by the various components of the oomycete and fungal PM, while the mutant StLTPa^{3A} protein is not (Figure 4f,g).

To further proof that StLTPa binds to the PM, instead of the cell wall of *P. infestans*, we performed cell wall binding assays. The results show that StLTPa does not bind to the cell wall of *P. infestans* (Figure 4h). To investigate whether StLTPa disturbs the functioning of the PM of the pathogen, we incubated zoospores of *P. infestans* with a 10 μM solution of the StLTPa protein for a period of 5 h and determined the integrity of the PM and viability of the zoospores by using the PM-impermeable DNA-binding dye propidium iodide (PI). PI cannot cross the PM of cells that are alive but can penetrate the cells and stain their nucleus when the PM is damaged. We observed that the PM of the

zoospores that were treated with GST-StLTPa were severely damaged, as these showed strong red fluorescence in their nucleus, while the GST-GFP- and GST-StLTPa^{3A} treated zoospores were fully intact and normally germinated (Figure 5a,b). Ion leakage assays revealed that the ion leakage of the GST-StLTPa-treated zoospores was significantly higher than the ion leakage of the zoospores that had been subjected to the control GST-GFP treatment (Figure 5c). In addition, the protoplasts of *P. infestans* treated with GST-StLTPa or GST-StLTPa^{3A} (5 μM) proteins were stained with FM4-64 dye, and 5 h after treatment we observed that StLTPa treatment resulted in increased membrane permeability indicated by the enhanced cytoplasmic staining of FM4-64, compared to StLTPa^{3A} treated samples (Figure 5d). Furthermore, we also observed at 5 hpi (hours post incubation) StLTPa induces a clear permeability of the *P. infestans* protoplasts and at 6 hpi the protoplasts collapsed completely, while StLTPa does not damage potato protoplasts at 5 hpi (Figure 5e; Figure S13). To test whether adding of lipids could compete the binding of StLTPa with *P. infestans* PM, we incubated GST-StLTPa, PI(3)P or PI(3,5)P₂ with protoplasts for 5 h, and ion leakage results show that adding of both PI(3)P or PI(3,5)P₂ reduced cytolytic activity of StLTPa in a phosphoinositide concentration-dependent manner (Figure 5f). The mycelium growth assays showing adding of 10*PI(3,5)P₂ or 10*PI(3)P compromised StLTPa mediated mycelium growth inhibition of *P. infestans* (Figure 5g,h). These results indicate that the lipid binding activity of StLTPa is essential for enhancing the permeability of the PM of the pathogen, and to thereby confer antimicrobial activity and trigger SNS BSR.

Here we report that the potato StLTPa protein has antimicrobial activity and enhances potato broad-spectrum disease resistance by binding to the lipids on the PM and perturbing the PM of the cells of various pathogens (Figure 5i).

Discussion

In this study we identified a potato StLTPa protein that enhances species none-specific broad-spectrum disease resistance against oomycete, fungal and bacterial pathogens (Figures 1–3). We provide evidence that StLTPa binds to lipids present in the PM of the hyphal cells of *P. infestans*, somehow leading to an increased permeability of its PM (Figures 4 and 5). Further investigations showed that the lipid-binding activity of StLTPa is essential for its role in pathogen inhibition and promotion of potato disease resistance to various pathogens (Figures 3 and 5). Our discovery illustrates that increasing the expression of a single gene in potato enhances broad-spectrum disease resistance (Figure 5).

The role of LTPs as antifungal and antibacterial proteins has been reported previously (Chen *et al.*, 2021a; McLaughlin *et al.*, 2021; Patkar and Chattoo, 2006). However, by which mechanism they confer this anti-microbial activity and whether they also confer anti-oomycete activity is not known. Here we provide evidence that StLTPa binds to the lipids present in the PM of *P. infestans*, thereby promoting its permeability (Figures 4 and 5). Besides, we also show that StLTPa inhibits the germination and growth of various microbial pathogens, such as the oomycete *P. infestans*, the fungus *B. cinerea* and the bacteria *P. carotovorum* and *R. solanacearum* (Figure 3). StLTPa does not bind to the PM of potato cells (Figure 4c,d; Figure S13), indicating that potato may have special mechanisms by which its PM is protected from being targeted and permeabilised by StLTPa.

Our study shows that an increased expression of StLTPa enhances potato SNS BSR (Figures 1 and 2). In most cases,

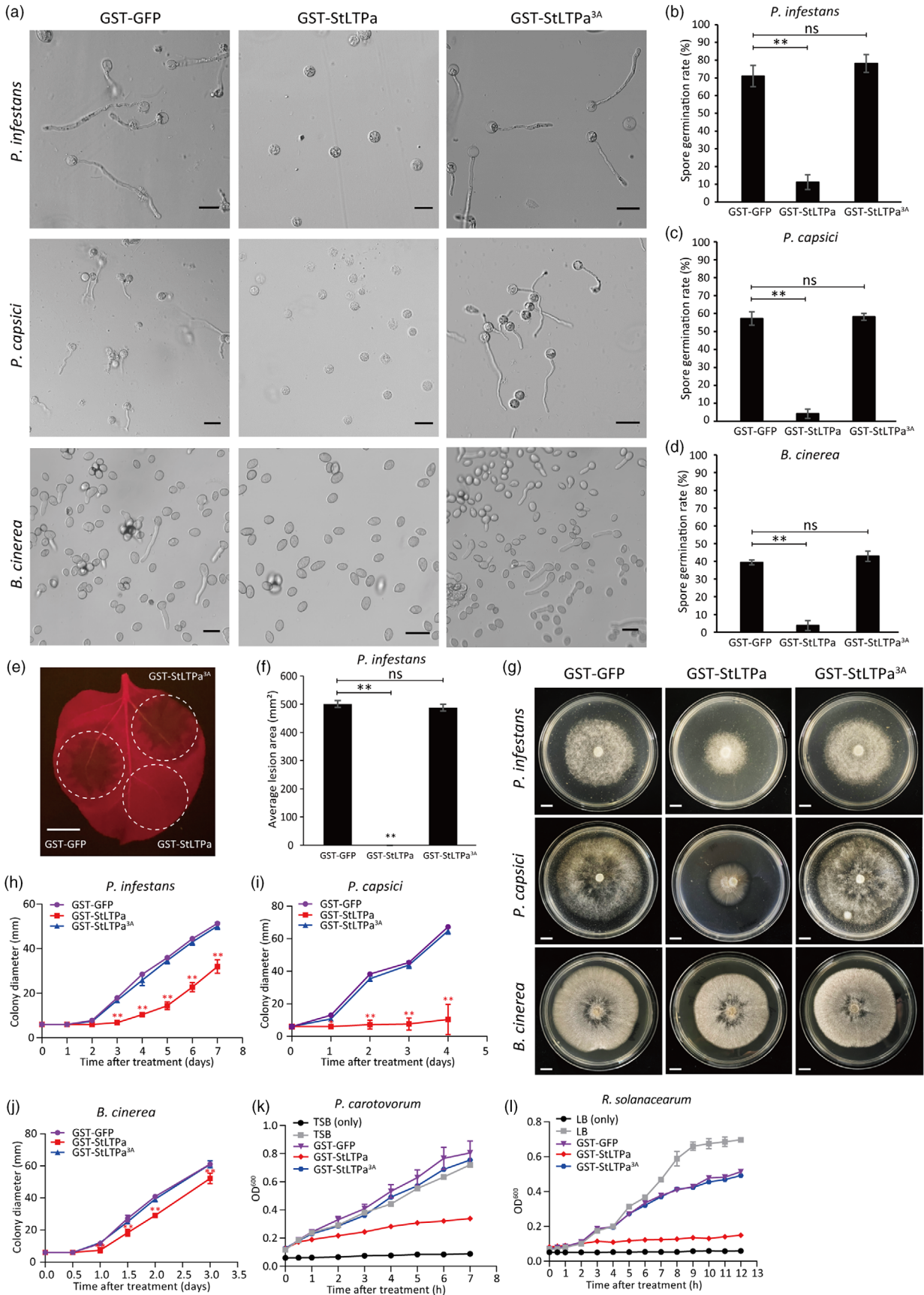


Figure 3 StLTPa inhibits pathogen germination and growth. (a) StLTPa inhibits spore germination of *P. infestans*, *P. capsici* and *B. cinerea*. Representative images were taken after 5 h of incubation with the GST-GFP control, GST-StLTPa and the GST-StLTPa^{3A} triple mutant, all at a concentration of 5 μ M. Scale bars, 20 μ m; for each treatment $n > 100$ spores were incubated. Bar graphs showing the spore germination rates for *P. infestans* (b), *P. capsici* (c), *B. cinerea* (d). Error bars indicate the standard error. Significance is indicated with asterisks ($n = 10$; one-sided Student's *t*-test, ** indicates $P < 0.01$, ns indicates non-significant differences). (e) Zoospores of *P. infestans* were incubated in a solution of 5 μ M of purified GST-GFP, GST-StLTPa and GST-StLTPa^{3A} proteins for 5 h, after which they were used to inoculate *N. benthamiana* leaves. Pictures showing lesion development on *N. benthamiana* leaves upon inoculation with zoospores of *P. infestans* were taken under blue light at 5 days after inoculation (dai). Scale bar, 1 cm. (f) Bar graph showing the average lesion areas on the inoculated leaves of which an example is shown in (e). Error bars indicate the standard error from 8 technical replicates. Significance is indicated with asterisks (one-sided Student's *t*-test, ** indicates $P < 0.01$, ns indicates non-significant differences). (g) GST-StLTPa inhibits radial growth of *P. infestans* Pi14-3-GFP, *P. capsici* BS11-1 and *B. cinerea* B05.10 strains at a concentration of 5 μ M, while the GST-StLTPa^{3A} and GST-GFP proteins do not affect radial growth. Images were taken at 7 days after inoculation of the plates with *P. infestans* and at 4 days after inoculation with *P. capsici* and at 3 days after inoculation with *B. cinerea*. Scale bar, 1 cm. Average colony diameters of *P. infestans* (h), *P. capsici* (i), *B. cinerea* (j), as measured over time. In (h–j), the error bars represent the standard deviations from at least five biological replicates. Significance is indicated with asterisks ($n \geq 5$, one-sided Student's *t*-test, * indicates $P < 0.05$, ** indicates $P < 0.01$). (k) Multiplication of *P. carotovorum* is inhibited by GST-StLTPa in TSB medium, while the GST-StLTPa^{3A} and GST-GFP proteins do not inhibit the multiplication of *P. carotovorum*. Graphs display the average OD₆₀₀ of *P. carotovorum* cultures from three biological replicates. (l) Multiplication of *R. solanacearum* is inhibited by StLTPa in LB medium. Graphs display the average OD₆₀₀ of *R. solanacearum* cultures incubated with the purified proteins GST-StLTPa, GST-StLTPa^{3A} and the control GST-GFP protein. In (k) and (l), the error bars represent standard deviations from three biological replicates. The experiment was repeated at least three times with similar results.

enhancement of disease resistance by up regulation of resistance genes or depletion of susceptibility genes is accompanied by compromised growth of crops. These growth-defence trade-offs can be attributed to the re-allocation of resources or competition of the regulating pathways between these two processes (Brown, 2003; Neuser *et al.*, 2019). However, there are exceptions, as plants are able to recruit beneficial microbes to improve their growth, fitness, stress response and yield (Compant *et al.*, 2019; Gao *et al.*, 2021). For example, *Trichoderma spp* are important bio-control fungi that promote plant growth and immunity through competition, the production of inhibitory secondary metabolites, heavy parasitism, and induction of disease resistance in various crops, such as melon, bean, tomato and rice (Evidente *et al.*, 2003; Gao *et al.*, 2021; Martínez-Medina *et al.*, 2014; Mayo *et al.*, 2015; Medeiros *et al.*, 2017; Nawrocka and Malolepsza, 2013).

The potato genome encodes more than 100 nSLTP proteins, and the subcellular localization of the various nSLTPs is diverse, as most of them are found in the apoplast, whereas others are found in the cell wall, the PM and the cytoplasm. Consequently, regarding their diverse subcellular localization, lipid-binding and lipid transfer capacity, and expression profiles, StLTPs must have evolved diverse mechanisms to regulate potato immune responses and growth. However, to date very few StLTPs have been studied in relation to their role in plant immunity and growth. A single report has been published on StLTP10, which was shown to interact with the ABA receptor PYRABACTIN RESISTANCE 1-LIKE 4 (PYL4) to regulate stomata closure and thereby enhance resistance of potato to *P. infestans* colonization (Wang *et al.*, 2021). Our research provides evidence that the up regulation of the expression of a single gene can enhance crop broad spectrum disease resistance. Our work also sets a good example for the breeding of BSR crops, without a penalty in growth.

Experimental procedures

Plasmid construction

For transient expression assays and stable transformations, the StLTPa (PGSC0003DMC400054441), StLTPb (PGSC0003DMC400003396) and StLTPc (PGSC0003DMC400021169) gene were

amplified from cDNA generated from potato cultivar Desiree and cloned into the pART27-CGFP vector using *Xho*I and *Hind*III sites, to generate the StLTPa-GFP, StLTPb-GFP and StLTPc-GFP plasmids. For potato transformation, targeted DNA fragment of StLTPa was cloned into the 35s-pART27 vector using *Xho*I and *Eco*RI sites, and the antisense DNA targeted fragment of StLTPa was cloned into the same vector using *Xba*I and *Hind*III sites to generate the RNA interference plasmid (StLTPa-RNAi). For the assessment of antimicrobial activity of the LTP protein, GFP, StLTPa and the triple mutant StLTPa^{R67AY102AI104A} were cloned into the pGEX-6p-1 vector using the *Bam*H1 and *Sal*I sites, to generate the GST-GFP, GST-StLTPa and GST-StLTPa^{R67AY102AI104A} plasmids, respectively. The primers that were used are listed in Table S2.

Agro-infiltration and VIGS

Agrobacterium tumefaciens strain C58C1, harbouring plasmids for expression *in planta*, was cultured at 28 °C in LB medium with the appropriate antibiotics, for 1 day. The bacteria were collected by centrifugation at 3000 *g* for 5 min, after which they were re-suspended in infiltration medium as described by Van der Hoorn *et al.* (2000). The optical density (OD) of the bacterial suspension was adjusted to an OD₆₀₀ of 0.3 for transient expression in *N. benthamiana*. For VIGS assays, a 343 bp sequence of the *NbLTP* gene was selected to generate the TRV-*NbLTP* plasmid. The TRV1 and TRV2-*NbLTP* plasmids were transformed into *Agrobacterium* strain C58C1 and the transformants were mixed in a 1 : 1 ratio to a final OD₆₀₀ of 0.6 for agroinfiltration. Two weeks old *N. benthamiana* seedlings were agroinfiltrated with TRV-*NbLTP* or TRV-*GUS*, and 3 weeks after agroinfiltration the silencing efficiency was determined by qRT-PCR, using the primers listed in Table S2.

Potato transformation

A. tumefaciens-harbouring StLTPa-GFP and StLTPa-RNAi were transformed into potato cv Desiree by stem segment transformation as described by Sun *et al.* (2016). The rooted transformants were transferred to MS medium without antibiotics in a climate chamber with a 16/8 h day/night cycle at 23 °C and incubated for 3 weeks, before being planted into plastic

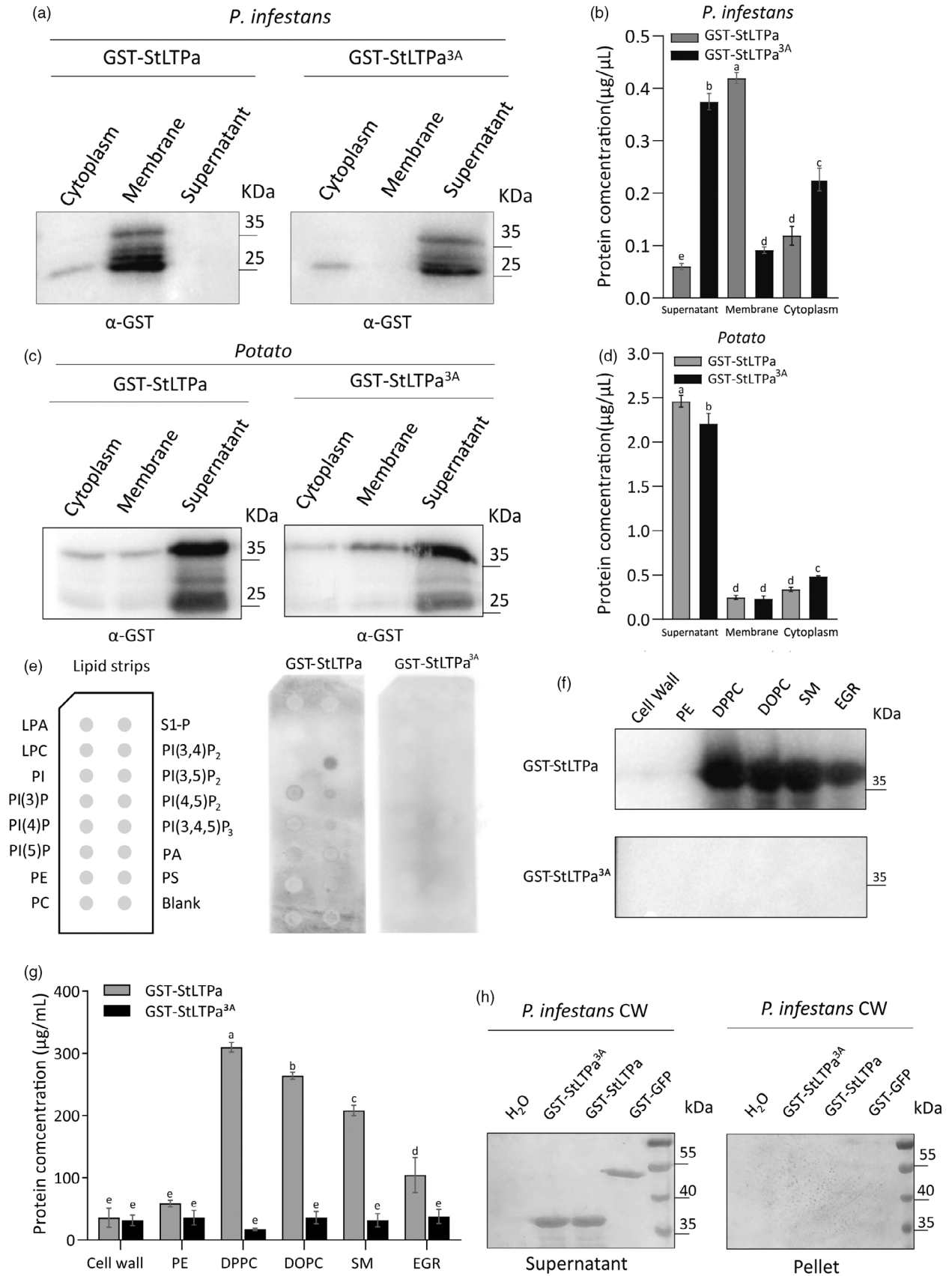


Figure 4 StLTPa binds to various lipids from plasma membrane. (a–d) StLTPa retention capability of various cell component of protoplasts assay. (a, c) Western blot analysis of the presence of GST-StLTPa and GST-StLTPa^{3A} protein in the cytoplasm, PM and supernatant fractions of protoplasts of *P. infestans* (a) and potato (c) respectively, which were detected using GST-antibodies. Bar graphs showing the concentration of GST-StLTPa and GST-StLTPa^{3A} in each fraction of the protoplasts of *P. infestans* (b) and potato (d), as determined from three biologically independent samples. Different letters indicate significantly different groups ($P < 0.05$, ANOVA, Tukey's HSD). The experiments were repeated at least two times with similar results. (e) Lipid binding properties of StLTPa in a protein/lipid overlay assay. GST-StLTPa and GST-StLTPa^{3A} were purified from *Escherichia coli* the proteins were incubated with a commercial PIP strip, after which anti-GST antibodies were used to detect bound GST-StLTPa or GST-StLTPa^{3A}. LPA, lysophosphatidic acid; LPC, lysophosphocholine; PI, phosphatidylinositol; PI(3)P, phosphatidylinositol (3)-phosphate; PI(4)P, phosphatidylinositol (4)-phosphate; PI(5)P, phosphatidylinositol (5)-phosphate; PE, phosphatidylethanolamine; PC, phosphatidylcholine; S1-P, sphingosine 1-phosphate; PI(3,4)P₂, phosphatidylinositol (3,4)-biphosphate; PI(3,5)P₂, phosphatidylinositol (3,5)-biphosphate; PI(4,5)P₂, phosphatidylinositol (4,5)-biphosphate; PI(3,4,5)P₃, phosphatidylinositol 3,4,5-triphosphate; PA, phosphatidic acid; PS, phosphatidylserine. The experiment was repeated twice with similar results. (f, g) Capability of various plasma membrane lipids of *P. infestans* to retain GST-StLTPa or GST-StLTPa^{3A}. Glass slides that had been coated with the indicated lipids were incubated with the GST-StLTPa and GST-StLTPa^{3A} proteins, and retained proteins were detected by Western blot using anti-GST antibodies (f). (g) The GST-StLTPa and GST-StLTPa^{3A} proteins were quantified by Coomassie brilliant blue (Bradford), in five technical replicates. Error bars show the standard errors. Different letters indicate significantly different groups ($P < 0.05$, ANOVA, Tukey's HSD). PE, phosphatidylethanolamine; DPPC, 1,2-dipalmitoyl-sn-glycero-3-phosphocholine; DOPC, 1,2-dioleoyl-sn-glycero-3-phosphocholine; SM, sphingomyelin; EGR, ergosterol. (h) Cell wall binding assay of *P. infestans* for recombinant GST-StLTPa and GST-StLTPa^{3A} proteins. H₂O, GST-StLTPa^{3A} or GST-StLTPa, GST-GFP proteins were incubated with an insoluble cell wall preparation of *P. infestans* strain Pi14-3-GFP, after which the suspensions were centrifuged. Subsequently, the supernatant and pellet phases were analysed for the presence of GST-GFP, GST-StLTPa and GST-StLTPa^{3A} proteins through SDS-PAGE, followed by Coomassie brilliant blue staining. Note that none of the proteins bind to the cell walls. The experiments were repeated three times with similar results.

pots. For testing the StLTPa transformation construct, more than five independent StLTPa-OE transformants and two StLTPa-RNAi transformants were obtained and confirmed by PCR and qRT-PCR, using the primers listed in Table S2.

Pathogen strains and growth conditions

Phytophthora infestans isolate 14-3-GFP was grown on RSA plates at 18 °C in the dark for approximately 2 weeks, before zoospores were collected. *P. capsici* isolate BS11-1 was grown on 5% carrot juice agar (CA) plates at 23 °C in the dark for 4–5 days, and the zoospores were prepared as described previously (Fan *et al.*, 2018). *Botrytis cinerea* strain B05.10 was grown on potato dextrose agar (PDA) plates in the dark at 23 °C for 3–4 days, before spores were collected. *Ralstonia solanacearum* strain GM1000 was grown in liquid LB medium overnight at 28 °C in a shaker at 200 rpm. *Verticillium dahliae* strain DVD-S26 was grown on PDA plates in the dark for 3–4 days before spores were collected. *Pectobacterium carotovorum* subsp. *Brasiliense* strain 212 was grown on tryptic soy agar in the dark at 28 °C for 1 day, after which the bacteria were cultured at 28 °C in tryptic soy broth (TSB) medium in a shaker at 200 rpm.

Plant growth conditions and pathogen inoculation assays

Potato and *N. benthamiana* were grown in a climate chamber with a 16/8 h day/night cycle at 25 °C. Four- to five-week-old *N. benthamiana* and 5-week-old potato plants were used for inoculation assays. For this, zoospores from *P. infestans* isolate 14-3-GFP were collected as described previously (Du *et al.*, 2021) and detached leaf assays were performed by inoculating 10 µL of a zoospore suspension, containing 1000 zoospores, onto one potato leaflet. The inoculated leaves were kept at 100% relative humidity in the dark at 18 °C and the lesion diameters were measured at 4 days after inoculation (dai). For *B. cinerea* inoculation, the spore suspension was prepared as described previously (Zhang and van Kan, 2013), and for each leaf, a 2 µL spore suspension that contained approximately 2000 spores was used. The inoculated leaves were kept in a box with 100% relative humidity at room temperature, and at 2 dai the lesion diameters were measured. For

P. carotovorum inoculation, overnight cultures of *P. carotovorum* subsp. *Brasiliense* strain 212 (Henan Agricultural University) in TSB medium were grown, and the bacteria were collected by centrifugation at 1000 g for 5 min, after which the bacteria were re-suspended in infiltration buffer (10 mM MgCl₂, 200 µM acetosyringone, 1 mM MES, pH 5.6) at an OD₆₀₀ of 0.1. For inoculation, the petioles from the 4th to 6th leaf positions of 5–6 weeks-old potatoes were soaked in the *P. carotovorum* suspensions. For *R. solanacearum* inoculation, overnight cultures were collected and washed two times before dilution with distilled tap water to an OD₆₀₀ of 0.1. Two-week-old potato plants were inoculated with *R. solanacearum* suspensions using the method described previously (Wang *et al.*, 2019). Wilting symptoms were determined at 5 dai, and the number of bacteria residing in the aerial parts of the infected plants (cfu/fresh weight) was counted as described previously. *V. dahliae* conidiospores were collected from 7 to 10 days-old cultures grown on PDA plates and washed with tap water. Disease assays were performed on potato plants using the root-dipping inoculation method, as previously described (Fradin *et al.*, 2009). Disease symptoms were photographed at 14 days post inoculation (dpi). For *V. dahliae* biomass quantification, stems from six inoculated plants were harvested at 14 dpi. The samples were ground into a fine powder in liquid nitrogen and genomic DNA was isolated. Real-time PCR was subsequently conducted by using the fungus-specific primers ITS-F and ST-VE1-R (Table S2).

Antimicrobial activity assays

To assay the effect of the StLTPa protein on the germination of zoospores from *P. infestans* and *P. capsici*, and spores from *B. cinerea*, *in vitro* bioassays were performed as described by Guevara *et al.* (2002). The spores were incubated with purified GST-StLTPa, GST-StLTPa^{3A} or GST-GFP protein for 5 h, and germination was observed using a differential interference contrast (DIC) microscope. For plate growth assays, *P. infestans*, *P. capsici*, and *B. cinerea*, were grown on RSA, CA, and PDA media, respectively, containing 5 µM concentration of GST-StLTPa, GST-StLTPa^{3A} and control GST-GFP proteins, and colony diameters were measured from at least five replicates. For *in vitro* bactericidal assays, *P. carotovorum* and *R. solanacearum* were

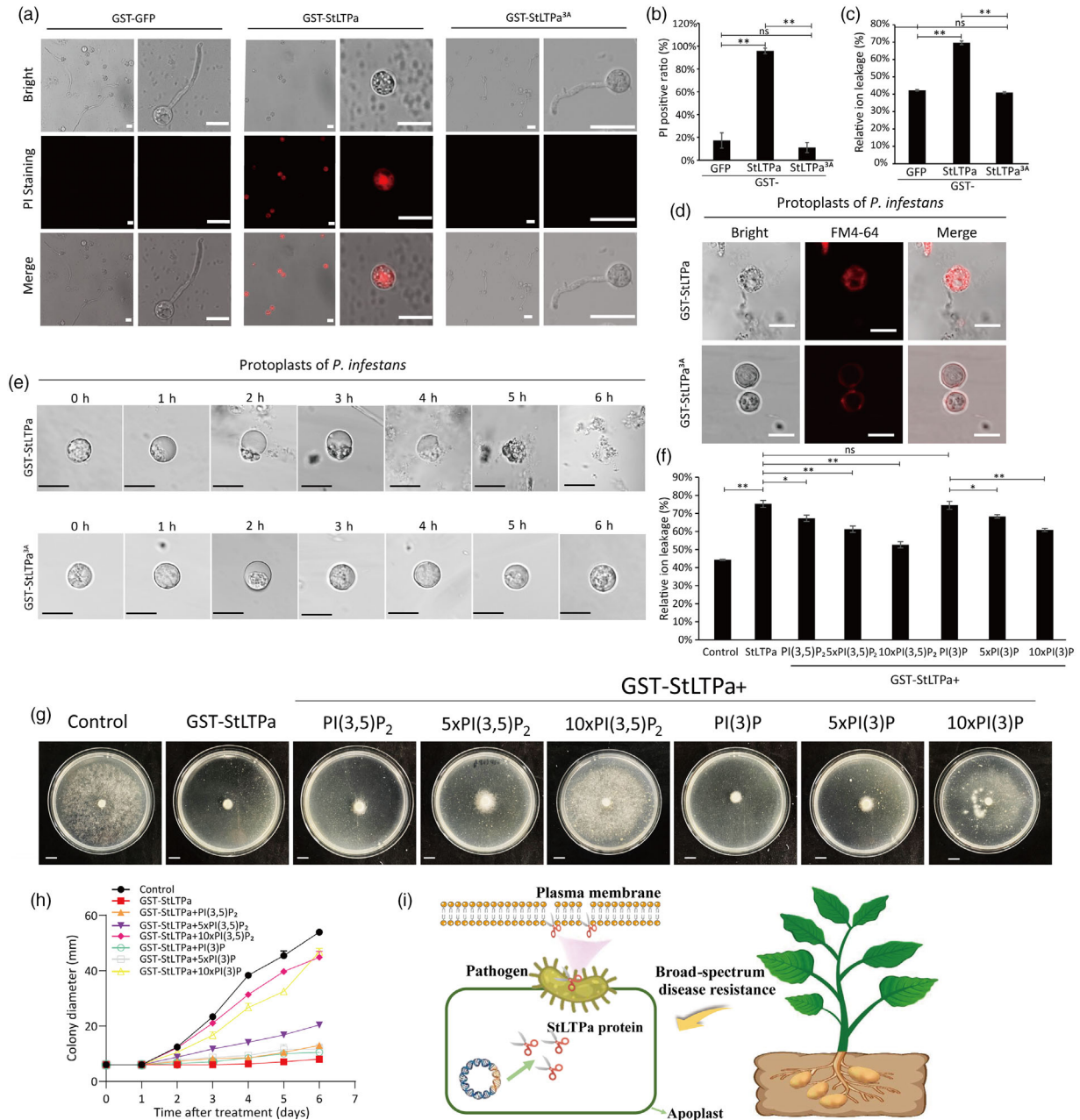


Figure 5 Lipid-binding activity is essential for the promotion of permeability of the plasma membrane of the cells and growth inhibition of pathogens. (a) Capability of the StLTPa protein to permeabilize the PM of spores of *P. infestans*. Spores of *P. infestans* were incubated with GST-GFP (left), GST-StLTPa (middle), and GST-StLTPa^{3A} (right) proteins at 10 μ M. Spores were then stained with propidium iodide (PI). Scale bars, 10 μ m. Representative images were taken after 5 h of incubation of $n > 100$ spores. (b) The percentage of *P. infestans* spores showing PI staining after the protein incubation as shown in (a). Bar graph showing the percentages of PI staining after the different incubations. Significance is indicated with asterisks ($n > 10$, one-sided Student's *t*-test, ** $P < 0.01$, ns indicates non-significant differences). (c) Quantification of ion leakage from *P. infestans* zoospores treated with the different proteins. Bar graph showing the relative ion leakage of the zoospores upon the treatment shown in (a). Error bars indicate the standard error from five technical replicates. Significance is indicated with asterisks (one-sided Student's *t*-test, ** $P < 0.01$, ns indicates non-significant differences). (d) Protoplasts of *P. infestans* treated with GST-StLTPa (5 μ M) or control GST-StLTPa^{3A} (5 μ M) were stained with FM4-64 dye and observed at the indicated timepoints after treatment. Scale bar, 10 μ m. (e) Representative images were taken after incubation of protoplasts of *P. infestans* with GST-StLTPa and GST-StLTPa^{3A} at a concentration of 5 μ M at different timepoints (0–6 h). Scale bars, 10 μ m. (f) Bar graph showing the relative ion leakage of protoplasts of *P. infestans* were co-incubated with GST-StLTPa and different concentration of PI(3, 5)P₂ or PI(3)P. Error bars indicate the standard error from 3 technical replicates. Significance is indicated with asterisks (one-sided Student's *t*-test, * $P < 0.05$, ** $P < 0.01$, ns indicates non-significant differences). (g) GST-StLTPa inhibits radial growth of *P. infestans* Pi14-3-GFP which was mitigated by PI(3)P and PI(3,5)P₂ in a concentration-dependent manner. Scale bars, 1 cm. (h) Average colony diameters of *P. infestans* (g) as measured over time. In (h), the error bars represent the standard deviations from at least four biological replicates. In (f–h), GST-GFP was used as a control. The experiment was repeated at least two times with similar results. (i) Proposed model for StLTPa-mediated broad-spectrum disease resistance. StLTPa is secreted by potato plants into the apoplast, and it binds to and perturbs, plasma membrane lipids of plant pathogens, thereby inhibiting pathogen growth.

grown in TSB and LB medium, respectively, at 28 °C with continuous shaking overnight at 200 rpm, before the bacteria were harvested by centrifugation at 3000 **g** for 5 min. The bacteria were then resuspended in the appropriate medium to an OD₆₀₀ of 0.1. A 5 μM solution of the StLTPa protein was co-incubated with the bacteria in a 96-well cell culture dish. The concentration of the bacteria (OD₆₀₀) was determined at 7 or 12 h after incubation for *P. carotovorum* or *R. solanacearum*, respectively, using a microplate reader.

Confocal microscopy imaging assay

To visualize PI-stained spores and FM4-64-stained protoplasts of the *P. infestans*, the fluorescence was observed using a confocal laser scanning microscope (Leica TCS-SP8 SR). RFP excitation was performed using a 552 nm solid-state laser, and fluorescence was detected at 590–640 nm, and the intensity and gain were 9.1% and 800, respectively. Pinholes were adjusted to 1 Airy Unit for each wavelength. Images were post-processed using the Leica LAS X software (Version 3.7.2) and ImageJ 1.8.0.

Apoplastic fluid isolation and LC–MS/MS analysis

Middle leaves of 4-week-old *N. benthamiana* plants were detached and inoculated at 30 positions for each leaf with *P. infestans* zoospore suspension (1000 zoospores per infection site). The leaves were harvested at 0 and 24 h post inoculation (hpi) for apoplastic fluid isolation, using the method as described by Joosten (2012). The collected apoplastic fluid was added to a 0.45 μM ultrafiltration tube in batches, centrifuged at 3000 **g** to remove impurities, and the protein-containing liquid was collected through the filtration membrane, and stored at –80 °C, after freeze drying. The proteins present in the apoplastic fluid were digested with trypsin and subjected to analysis by high-sensitivity LC–MS/MS, using a QExactive HF-X spectrometer (ThermoFisher, Waltham, MA).

PIP strip assay

Lipid-binding assays were performed using a PIP strip (Echelon Biosciences, catalogue no. P-6001), following a protocol described previously (Casamayor and Snyder, 2003). GST-StLTPa and GST-StLTPa^{3A} constructs were transformed to *Escherichia coli* strain BL21-CodonPlus (DE3) and the produced proteins were purified as described by Li *et al.* (2014). The PIP strip membrane was blocked for 1 h at room temperature with a PIP strip blocking buffer containing 10 mM Tris (pH 7.4), 150 mM NaCl, 3% fatty acid-free bovine serum albumin and 0.1% (v/v) Tween-20. The PIP strip was then incubated with approximately 2 μg of GST-StLTPa or GST-StLTPa^{3A} protein in 5 mL of fresh PIP strip blocking buffer, overnight at 4 °C. After washing three times (for 10 min each), bound proteins on the strip were incubated for 1 h with a GST antibody (#AE006, ABclonal), diluted at 2000 times in the PIP strip wash buffer. The strip was then washed three times and incubated with the secondary antibody HRP goat anti-mouse IgG (H + L) antibody (#AS003, ABclonal) for 1 h. The PIP strip membranes were developed using a chemiluminescence western kit (CWBIO, Beijing, China) and visualized in a ChemiDoc XRS+ Imaging System (Bio-Rad).

Proteins molecule retention assay

The StLTPa molecule retention assay was performed as described earlier (Song *et al.*, 2019). First, protoplasts of *P. infestans* and potato were prepared according to previous reports (Fang *et al.*, 2017; Yoo *et al.*, 2007), and the protoplasts were subsequently incubated with the GST-StLTPa and GST-StLTPa^{3A} proteins. Then, cells and

supernatants were collected separately by centrifugation (100 **g** for 5 min) and the protoplasts were treated with buffer A (20 mM Tris–HCl, 2 mM EDTA, 1 mM dithiothreitol and 10% glycerol) on ice to disrupt the PM. Cytosol and membrane fragments were separated by ultracentrifugation (17 000 **g** for 20 min, at 4 °C). The membrane fragments were subsequently dissolved in buffer B (buffer A with 1% Triton X-100). StLTPa in the fractions was dried by rotary evaporation and resolved with DMSO in equivalent volumes and subsequently detected using the Western blot using α-GST antibodies. The amount of StLTPa present in each sample was quantified by Coomassie brilliant blue G250 (Bradford). The binding ability of the StLTPa protein to various lipids was analysed using a lipid-binding assay (Song *et al.*, 2019; Xu *et al.*, 2022). For this, 1 mg/mL of each lipid species was dissolved in chloroform and was coated on round glass slides by evaporation. Then, the glass slides were incubated with 10 μM GST-StLTPa or GST-StLTPa^{3A} protein in dimethyl sulfoxide (DMSO) (1%), with 0.01 M PBS, at 37 °C. After the incubation, the glass slides were washed with PBS for five times and the lipids were dissolved in DMSO. The binding ability of StLTPa to the various lipids present in each sample was subsequently determined by Western blotting using α-GST antibodies. The amount of StLTPa in each sample was measured by Coomassie brilliant blue G250 (Bradford). The lipids PE (1535744), DOPC (850375), DPPC (850355) (Avanti Polar Lipids), SM (860061) and ergosterol (45480, Sigma-Aldrich) were used. The relative amount of StLTPa was calculated from five technical replicates.

Cell wall preparations

P. infestans isolate 14-3-GFP were culture in liquid Rye-sugure medium at 18 °C in the dark for 9 days. The mycelium were harvested for protein-free cell wall isolation as described by Wawra *et al.* (2016). Prior to use, the obtained polysaccharide pellet was ground to a fine powder.

For cell wall polysaccharide pull down assays, 50 mg of *P. infestans* cell wall powder was weighted into sterilized centrifuge tubes and 600 μL of water was added. The polysaccharides were then sonicated for 30 s before the addition of 300 μL of protein solution of either 20 μM GST-StLTPa or GST-StLTPa^{3A}, to obtain a final buffer condition of 10 mM sodium acetate pH 5.0, containing 300 mM NaCl. The mixture was incubated for 1 h at room temperature before centrifugation for 10 min at 12 000 **g**. Supernatant fractions were obtained by removal of 600 μL clear protein solution that was precipitated with 500 μL 40% trichloroacetic acid, overnight at 4 °C. The supernatant samples were centrifuged for 30 min at 12 000 **g** (4 °C) and the pellets were washed three times with 100% acetone before drying. SDS-PAGE samples were obtained by boiling the samples for 5 min at 100 °C with 100 μL of Laemmli SDS sample buffer (8 M urea, 2 M thiourea) and 20 μL of each sample were loaded onto SDS-PAGE gels for analysis.

Gene expression assays

Plant total RNAs were extracted by using the RNA Kit (TianGen, Beijing, China, Cat No. DP419). cDNA was synthesized using a Real-Time Kit for qPCR (Accurate Biology, Hunan, China, Cat No. AG11705). *Stactin* (XM_006350963) and *Nbactin* were used as reference genes in potato and *N. benthamiana*, respectively, for normalization (Chen *et al.*, 2021b).

Accession numbers

Accession numbers are as follows: StLTPa, PGSC0003DMP4000 54441; StLTPb, PGSC0003DMP400003396; StLTPc, PGSC000

3DMP400021169; StLTPd, PGSC0003DMP400022245; StLTPe, PGSC0003DMP400044290; StLTPf, PGSC0003DMP400044288; StLTPg, PGSC0003DMP400022731; StLTP2, PGSC0003DMP400010171; AtLTP1, At2g38540; AtLTP2, At2g38530; AtLTP2.1, At1g43665; NbLTPa, Niben101Scf12307g01004; NbLTPb, Niben101Scf07809g00010; NbLTPc, Niben101Scf02655g01005; NbLTPd, Niben101Scf02335g03005; NbLTPe, Niben101Scf04600g00005; NbLTPf, Niben101Scf02655g01009; SILTPa, Solyc10g075050; SILTPb, Solyc09g018010; SILTPc, Solyc10g075110; SILTPd, Solyc10g075107; CaLTPI, Ca10g08490; CaLTPII, Ca10g12060; CaLTPIII, Ca06g12690; NtLTP1, BAK19105; OsLTP1.4, Os05g40010; OsLTP1.5, Os06g06340; OsLTP2.1, Os01g49640; OsLTP2.2, Os01g49650.

Acknowledgements

We would like to thank the Horticulture Science Research Center of Northwest A&F University for providing their advanced facilities and Dr. Qiong Zhang and Technician Xiaona Zhou of CSBAA for assistance with high-sensitivity LC–MS/MS (QExactive HF-X, Thermo Fisher, Waltham). We are grateful to Miss Beibei He and Jia Luo (Horticultural Science Research Center Northwest A&F University, Yangling, China) for providing professional technical assistance with microscope analysis and with the refrigerated centrifuge. We would like to thank Prof. Jun Zhao (Inner Mongolia Agricultural University) for sharing *Verticillium dahliae* strain DVD-S26; Prof. Francine Govers (Wageningen University) for sharing *P. infestans* isolates 88069, 14-3-GFP and T30-4; Dr. Kaile Sun (Henan Agricultural University) for sharing *P. carotovorum* subsp. *Brasiliense* strain 212; Dr. Haibin Lu for sharing *Ralstonia solanacearum* strain GM11000.

Funding

This work was supported by the National Science Foundation of China (32072401; 32372502), the Chinese Universities Scientific Fund (2452018028 and 2452017069), the Guizhou Provincial Basic Research Program (Natural Science) (ZK[2023]-096).

Conflict of interest

The authors declare no conflict of interest.

Author contributions

Y.D. designed the research. X.C., J.F., Z.L., performed the experiments. X.C. analysed the data. Y.D., X.C. wrote the manuscript. M.H.A.J.J., C.S., and L.C. revised the manuscript. H.F. and L.C. draw the model, and helped with planting of potato materials. All authors reviewed the manuscript.

Data availability statement

Data sharing is not applicable as no new data were created or analysed in this study.

References

Brown, J. (2003) A cost of disease resistance: paradigm or peculiarity? *Trends Genet.* **19**, 667–671.
 Casamayor, A. and Snyder, M. (2003) Molecular dissection of a yeast septin: distinct domains are required for septin interaction, localization, and function. *Mol. Cell. Biol.* **23**, 2762–2777.

Chen, B., Zhang, Y., Sun, Z., Liu, Z., Zhang, D., Yang, J., Wang, G. et al. (2021a) Tissue-specific expression of GhnsLTPs identified via GWAS sophisticatedly coordinates disease and insect resistance by regulating metabolic flux redirection in cotton. *Plant J.* **107**, 831–846.
 Chen, X., Wang, W., Cai, P., Wang, Z., Li, T. and Du, Y. (2021b) The role of the MAP kinase-kinase protein StMKK1 in potato immunity to different pathogens. *Hortic. Res.* **8**, 117.
 Cheng, H., Cheng, P., Peng, P., Lyu, P. and Sun, Y. (2004) Lipid binding in rice nonspecific lipid transfer protein-1 complexes from *Oryza sativa*. *Protein Sci.* **13**, 2304–2315.
 Compant, S., Samad, A., Faist, H. and Sessitsch, A. (2019) A review on the plant microbiome: ecology, functions, and emerging trends in microbial application. *J. Adv. Res.* **19**, 29–37.
 Du, Y., Stegmann, M. and Misas, J.C. (2016) The apoplast as battleground for plant–microbe interactions. *New Phytol.* **209**, 34–38.
 Du, Y., Chen, X., Guo, Y., Zhang, X., Zhang, H., Li, F., Huang, G. et al. (2021) *Phytophthora infestans* RXLR effector PITG20303 targets a potato MKK1 protein to suppress plant immunity. *New Phytol.* **229**, 501–515.
 Evidente, A., Cabras, A., Maddau, L., Serra, S., Andolfi, A. and Motta, A. (2003) Viridepyronone, a new antifungal 6-substituted 2H-pyran-2-one produced by *Trichoderma viride*. *J. Agric. Food Chem.* **51**, 6957–6960.
 Fan, G., Yang, Y., Li, T., Lu, W., Du, Y., Qiang, X., Wen, Q. et al. (2018) A *Phytophthora capsici* RXLR effector targets and inhibits a plant PPLase to suppress endoplasmic reticulum-mediated immunity. *Mol. Plant*, **11**, 1067–1083.
 Fang, Y., Cui, L., Gu, B., Arredondo, F. and Tyler, B.M. (2017) Efficient genome editing in the Oomycete *Phytophthora sojae* using CRISPR/Cas9. *Curr. Protoc. Microbiol.* **44**, 21A.1.1–21A.1.26.
 Fradin, E., Zhang, Z., Juarez, A.J., Castroverde, C., Nazar, R., Robb, J., Liu, C.M. et al. (2009) Genetic dissection of *Verticillium* wilt resistance mediated by tomato Ve1. *Plant Physiol.* **150**, 320–332.
 Gao, S., Guo, W., Feng, W., Liu, L., Song, X., Chen, J., Hou, W. et al. (2016) LTP3 contributes to disease susceptibility in *Arabidopsis* by enhancing abscisic acid (ABA) biosynthesis. *Mol. Plant Pathol.* **17**, 412–426.
 Gao, Y., Ning, Q., Yang, Y., Liu, Y., Niu, S., Hu, X., Pan, H. et al. (2021) Endophytic *Streptomyces hygrosopicus* OsiSh-2-mediated balancing between growth and disease resistance in host rice. *MBio*, **12**, e0156621.
 Gao, H., Ma, K., Ji, G., Pan, L. and Zhou, Q. (2022) Lipid transfer proteins involved in plant–pathogen interactions and their molecular mechanisms. *Mol. Plant Pathol.* **23**, 1815–1829.
 Ghislain, M., Byarugaba, A.A., Magembe, E., Njoroge, A., Rivera, C., Román, M.L., Tovar, J.C. et al. (2019) Stacking three late blight resistance genes from wild species directly into African highland potato varieties confers complete field resistance to local blight races. *Plant Biotechnol. J.* **17**, 1119–1129.
 Guevara, M.G., Oliva, C.R., Huarte, M. and Daleo, G.R. (2002) An aspartic protease with antimicrobial activity is induced after infection and wounding in intercellular fluids of potato tubers. *Eur. J. Plant Pathol.* **108**, 131–137.
 Hao, Z., Tian, J., Fang, H., Fang, L., Xu, X., He, F., Li, S. et al. (2022) A VQ-motif-containing protein fine-tunes rice immunity and growth by a hierarchical regulatory mechanism. *Cell Rep.* **40**, 111235.
 Joosten, M.H.A.J. (2012) Isolation of apoplastic fluid from leaf tissue by the vacuum infiltration-centrifugation technique. *Methods Mol. Biol.* **835**, 603–610.
 Joosten, M.H. and De Wit, P.J. (1989) Identification of several pathogenesis-related proteins in tomato leaves inoculated with *Cladosporium fulvum* (syn. *Fulvia fulva*) as 1,3-beta-glucanases and chitinases. *Plant Physiol.* **89**, 945–951.
 Ke, Y., Deng, H. and Wang, S. (2017) Advances in understanding broad-spectrum resistance to pathogens in rice. *Plant J.* **90**, 738–748.
 Lee, J.Y., Min, K., Cha, H., Shin, D.H., Hwang, K.Y. and Suh, S.W. (1998) Rice non-specific lipid transfer protein: the 1.6 Å crystal structure in the unliganded state reveals a small hydrophobic cavity. *J. Mol. Biol.* **276**, 437–448.
 Li, L., Li, M., Yu, L., Zhou, Z., Liang, X., Liu, Z., Cai, G. et al. (2014) The FLS2-associated kinase BIK1 directly phosphorylates the NADPH oxidase RbohD to control plant immunity. *Cell Host Microbe*, **15**, 329–338.
 Martínez-Medina, A., Del Mar Alguacil, M., Pascual, J.A. and Van Wees, S.C. (2014) *Phytohormone* profiles induced by *Trichoderma* isolates correspond

- with their biocontrol and plant growth-promoting activity on melon plants. *J. Chem. Ecol.* **40**, 804–815.
- Mayo, S., Gutierrez, S., Malmierca, M.G., Lorenzana, A., Campelo, M.P., Hermosa, R. and Casquero, P.A. (2015) Influence of *Rhizoctonia solani* and *Trichoderma* spp. in growth of bean (*Phaseolus vulgaris* L.) and in the induction of plant defense-related genes. *Front. Plant Sci.* **6**, 685.
- McLaughlin, J.E., Darwish, N.I., Garcia-Sanchez, J., Tyagi, N., Trick, H.N., McCormick, S., Dill-Macky, R. et al. (2021) A lipid transfer protein has antifungal and antioxidant activity and suppresses *Fusarium* Head Blight disease and DON accumulation in transgenic wheat. *Phytopathology*, **111**, 671–683.
- Medeiros, H.A., Araujo, F.J.V., Freitas, L.G., Castillo, P., Rubio, M.B., Hermosa, R. and Monte, E. (2017) Tomato progeny inherit resistance to the nematode *Meloidogyne javanica* linked to plant growth induced by the biocontrol fungus *Trichoderma atroviride*. *Sci. Rep.* **7**, 40216.
- Nawrocka, J. and Malolepsza, U. (2013) Diversity in plant systemic resistance induced by *Trichoderma*. *Biol. Control*, **67**, 149–156.
- Neuser, J., Metzgen, C.C., Dreyer, B.H., Feulner, C., van Dongen, J.T., Schmidt, R.R. and Schippers, J.H.M. (2019) HBI1 mediates the trade-off between growth and immunity through its impact on apoplastic ROS homeostasis. *Cell Rep.* **28**, 1670–1678.
- Patkar, R.N. and Chattoo, B.B. (2006) Transgenic indica rice expressing ns-LTP-like protein shows enhanced resistance to both fungal and bacterial pathogens. *Mol. Breed.* **17**, 159–171.
- Safi, H., Saibi, W., Alaoui, M.M., Hmyene, A., Masmoudi, K., Hanin, M. and Brini, F. (2015) A wheat lipid transfer protein (TdLTP4) promotes tolerance to abiotic and biotic stress in *Arabidopsis thaliana*. *Plant Physiol. Biochem.* **89**, 64–75.
- Schmitt, A.J., Sathoff, A.E., Holl, C., Bauer, B., Samac, D.A. and Carter, C.J. (2018) The major nectar protein of *Brassica rapa* is a non-specific lipid transfer protein, BrLTP2.1, with strong antifungal activity. *J. Exp. Bot.* **69**, 5587–5597.
- Sha, G., Sun, P., Kong, X., Han, X., Sun, Q., Fouillen, L., Zhao, J. et al. (2023) Genome editing of a rice CDP-DAG synthase confers multipathogen resistance. *Nature*, **618**, 1017–1023.
- Song, D., Meng, J., Cheng, J., Fan, Z., Chen, P., Ruan, H., Tu, Z. et al. (2019) *Pseudomonas aeruginosa* quorum-sensing metabolite induces host immune cell death through cell surface lipid domain dissolution. *Nat. Microbiol.* **4**, 97–111.
- Sun, K., Wolters, A.M.A., Vossen, J.H., Rouwet, M.E., Loonen, A.E.H.M., Jacobsen, E., Visser, R.G.F. et al. (2016) Silencing of six susceptibility genes results in potato late blight resistance. *Transgenic Res.* **25**, 731–742.
- Van der Hoorn, R.A.L., Laurent, F., Roth, R. and De Wit, P.J.G.M. (2000) Agroinfiltration is a versatile tool that facilitates comparative analyses of Avr9/Cf-9-induced and Avr4/Cf-4-induced necrosis. *Mol. Plant-Microbe Interact.* **13**, 439–446.
- Wang, H., Hu, J., Lu, Y., Zhang, M., Qin, N., Zhang, R., He, Y. et al. (2019) A quick and efficient hydroponic potato infection method for evaluating potato resistance and *Ralstonia solanacearum* virulence. *Plant Methods*, **15**, 145.
- Wang, C., Gao, H., Chu, Z., Ji, C., Xu, Y., Cao, W., Zhou, S. et al. (2021) A nonspecific lipid transfer protein, StLTP10, mediates resistance to *Phytophthora infestans* in potato. *Mol. Plant Pathol.* **22**, 48–63.
- Wang, N., Tang, C., Fan, X., He, M., Gan, P., Zhang, S., Hu, Z. et al. (2022) Inactivation of a wheat protein kinase gene confers broad-spectrum resistance to rust fungi. *Cell*, **185**, 2961–2974.
- Wang, D., Song, J., Lin, T., Yin, Y., Mu, J., Liu, S., Wang, Y. et al. (2023) Identification of potato lipid transfer protein gene family and expression verification of drought genes *StLTP1* and *StLTP7*. *Plant Direct*, **7**, e491.
- Wawra, S., Fesel, P., Widmer, H., Timm, M., Seibel, J., Leson, L., Kessler, L. et al. (2016) The fungal-specific β -glucan-binding lectin FGB1 alters cell-wall composition and suppresses glucan-triggered immunity in plants. *Nat. Commun.* **7**, 13188.
- Xu, S., Liu, Y.X., Cernava, T., Wang, H., Zhou, Y., Xia, T., Cao, S. et al. (2022) *Fusarium* fruiting body microbiome member *Pantoea agglomerans* inhibits fungal pathogenesis by targeting lipid rafts. *Nat. Microbiol.* **7**, 831–843.
- Yoo, S.D., Cho, Y.H. and Sheen, J. (2007) *Arabidopsis* mesophyll protoplasts: a versatile cell system for transient gene expression analysis. *Nat. Protoc.* **2**, 1565–1572.
- Zhang, L. and van Kan, J.A. (2013) *Botrytis cinerea* mutants deficient in D-galacturonic acid catabolism have a perturbed virulence on *Nicotiana benthamiana* and *Arabidopsis*, but not on tomato. *Mol. Plant Pathol.* **14**, 19–29.
- Zhang, H., Xu, F., Wu, Y., Hu, H.H. and Dai, X.F. (2017) Progress of potato staple food research and industry development in China. *J. Integr. Agric.* **16**, 2924–2932.

Supporting information

Additional supporting information may be found online in the Supporting Information section at the end of the article.

Table S1 Mass spectrometry datasheet of the proteins of which the accumulation is potentially induced in potato leaves upon inoculation by *P. infestans*

Figure S1 Identification of LTP proteins by LC–MS/MS.

Figure S2 NbLTP expression promotes resistance to *P. infestans* in *N. benthamiana*.

Figure S3 Silencing of *NbLTPa&b* facilitates *P. infestans* colonization.

Figure S4 Phylogenetic analysis of LTP proteins in potato, tomato, *Arabidopsis thaliana*, pepper, *Nicotiana benthamiana* and *Oryza sativa*.

Figure S5 Multiple amino acid sequence alignment of StLTP1-homologous proteins from *A. thaliana* and several *solanaceous* plants.

Figure S6 StLTPs expression promotes resistance to *P. infestans* in *N. benthamiana*.

Figure S7 Stable transgenic StLTPa overexpressing (OE) potato lines show increased plant growth and resistance.

Figure S8 Expression pattern of the *StLTPa* gene in response to *P. infestans* inoculation.

Figure S9 Silencing of StLTPa promotes *B. cinerea* and *R. solanacearum* colonization of potato plants.

Figure S10 StLTPa-GFP is localized in the apoplast of plants.

Figure S11 GST-StLTPa-treated *P. capsici* zoospores and *B. cinerea* spores are less virulent on leaves of *N. benthamiana* than when treated with GST-GFP.

Figure S12 Overexpression of StLTPa^{3A} does not enhance plant immunity to *P. infestans*.

Figure S13 StLTPa does not damage the plasma membrane (PM) of potato.

Table S2 Sequence of the primers used in this study